

Compilation of a harmonized point collection of the vertical deformation component from the 7.6 Mw Limón Earthquake of 1991 in Costa Rica and a comparison with the current state of deformation

Compilação de uma coleção de pontos harmonizada do componente de deformação vertical do terremoto de Limón de magnitude 7,6 ocorrido em 1991 na Costa Rica, e uma comparação com o estado atual de deformação

Jaime Garbanzo León¹ , César Hernández Jiménez¹ , Alonso Vega Fernández¹ ,
Mauricio Varela Sánchez¹ , Juan McGregor Sanabria¹ , Oscar Lücke² 

¹ University of Costa Rica, Surveying Engineering department. Ciudad de la Investigación, 11501, San Pedro, Costa Rica. (jaime.garbanzoleon@ucr.ac.cr; cesar.hernandezjimenez@ucr.ac.cr; alonso.vega_f@ucr.ac.cr; mauricio.varelasanchez@ucr.ac.cr; juan.mcgregor@ucr.ac.cr)

² GEOMAR Helmholtz Centre for Ocean Research Kiel - Kiel, Germany. (olucke@geomar.de)

Received on July 14, 2025; accepted on January 14, 2026.

ABSTRACT

The Limón earthquake that occurred on April 22, 1991, was one of the largest disasters recorded in Costa Rica, resulting in significant uplift on the Caribbean coast. After the earthquake, there have been several investigations into the surface deformations caused by the main shock. However, there is just one instance where researchers tried to gather a homogeneous deformation dataset from the other studies. In our study, we carried out a deeper investigation into several historical sources that report deformations to fill the information gap. Also, we tested the possibility of using the Costa Rica height system to expand the area of coverage, especially at the epicenter and deeper inland. As a result, we gathered 113 observations from 7 different sources, which dated from the date of the 1991 event to 1999. Furthermore, deformation data at 16 benchmarks from the Costa Rican height network were gathered from different studies and new observations. Most of the benchmarks show a positive deformation for the vertical component even when deformation measurements were carried out 30 years after the earthquake.

Keywords: Uplift; Earthquake; Co-seismic deformation; Post-seismic relaxation; Vertical component.

RESUMO

O terremoto de Limón, ocorrido em 22 de abril de 1991, foi um dos maiores desastres registrados na Costa Rica, resultando em soerguimento significativo na costa caribenha. Após o terremoto, foram realizadas várias investigações sobre as deformações superficiais causadas pelo evento principal. No entanto, há apenas um caso em que os pesquisadores tentaram reunir um conjunto de dados de deformação homogênea dos outros estudos. Em nosso estudo, realizamos uma investigação aprofundada em várias fontes históricas que relatam deformações para preencher a lacuna de informação. Além disso, testamos a possibilidade de usar o sistema de altura da Costa Rica para expandir a área de cobertura, especialmente no epicentro e mais para o interior. Como resultado, reunimos 113 observações de 7 fontes diferentes, que datam da data do evento 1991 até 1999. Além disso, dados de defor-

mação em 16 benchmarks da rede de altura da Costa Rica foram coletados de diferentes estudos e novas observações. A maioria dos benchmarks mostra uma deformação positiva para o componente vertical, mesmo quando as medições de deformação foram realizadas 30 anos após o terremoto.

Palavras-chave: Elevação; Terremoto; Deformação co-sísmica; Relaxamento pós-sísmico; Componente vertical.

INTRODUCTION

The Limón earthquake occurred on April 22nd, 1991, in the Caribbean Zone of Costa Rica at an estimated depth of 10 km. It derived its name because of the epicenter's proximity to the City of Puerto Limón and reached a 7.6 Mw magnitude (U.S. Geological Survey, 2014). This was produced by a fault, which is not exposed on land and extends offshore (Plafker and Ward, 1992). From the focal mechanism solution provided by GCMT (Dziewonski et al., 1981; Ekström et al., 2012), we observe a nodal plane (NP1) with a 103° strike, 25° dip, and a 58° rake and the second nodal plane (NP2) with a 318° strike, 69° dip and 104° rake. From these planes, based on regional tectonic features such as the characteristics of the North Panama Deformed Belt (Adamek et al., 1988), we consider NP1 to be the actual fault plane. This indicates an oblique-reverse faulting with a dominant thrust component and subordinate right-lateral motion. On the other hand, this event represented a major disaster, resulting in severe infrastructure damage, including the collapse of multiple bridges and communication disruption with the capital (Rodríguez-Roblero et al., 2021; Sauter, 1994).

Also, 12% of the total area of Costa Rica was affected (Quesada-Román, 2016) and it was reported as one of the biggest earthquakes in the world for that year (U.S. Geological Survey, n.d.). Because of the importance of this event, there has been a lot of independent efforts on assessing the different effects such as infrastructure damage, landslides, and earth crust deformation (Barrantes et al., 2021). One of the most dramatic effects of the earthquake was the uplift, which was evident at the coast exposing coral reef platforms along popular Caribbean beaches. Deformation is of importance to the scientific community because it gives us information about tectonic processes such as faults slip and potential recurrences. The deformation caused by such large earthquakes may be divided in two temporal and mechanical components: instantaneous co-seismic rupture and long-term post-seismic stress relaxation (Fu et al., 2025). This last one has been shown to decay between a range of 2 – 2.5 years (Ozawa et al., 2012; Yamagiwa et al., 2015). For this earthquake, co-seismic subsidence and

tectonic uplift instances were documented in the order of 0.01 to 1.0 m and 0.15 to 1.85 m respectively in several papers (Amador et al., 1994; Denyer et al., 1994; Lundgren et al., 1993; Plafker and Ward, 1992) but the magnitude of permanent deformation in the vertical component remains to be determined. Furthermore, the most likely explanation for subsidence is liquefaction.

For instance, Quesada-Román (2016) reported liquefaction near the Caribbean coast and BMs measure by Obaldía et al. (1991) showed negative deformation values near rivers and bridges. Moreover, just a few researchers have focused on integrating all the independent measurements to create a comprehensive dataset and a deformation model (Chacón-Barrantes and Zamora, 2017). However, none of them has evaluated the accuracy of each data point based on the equipment and methodology used to gather the data (i.e. the survey technique). On the other hand, there were efforts in Costa Rica to establish a new geodetic coordinate framework, with GNSS survey campaigns starting in 1990 and continuing until 1997 (Dörries and Roldán, 1999; Monge, 1991; Niemeier et al., 1993). These surveys contain the deformation signal considered as noise at the time for the geodetic framework aims. For instance, the network adjustments of CoRBas90 and CoRBas91, measured before the event, showed discrepancies of up to 1.6 m when compared to adjustments of the networks CoRBas 93 and TERRA, measured after the event. Therefore, the former geodetic networks were used as the basis for the CR98 geodetic datum (Dörries and Roldán, 2004). Recently, there have been efforts to generate a local and accurate geoid named GCR_RSH_2020 (Garbanzo-León et al., 2020), which serves as reference for the height system.

Geoid models allow the transformation from geometric heights (GNSS measurements) to physical height, such as the ones represented by the current Costa Rican altimetric system, and thus, this conversion makes the comparison possible. Moreover, Cordero and Lara (2023) conducted a search of benchmarks (BMs) belonging to Costa Rican altimetric system and concluded that it is not properly maintained, thus many of these BMs are destroyed or lost. In this search, they found several benchmarks located on the Caribbean Coast, within the area affected by the earthquake. On

the other hand, there are not many deformation datapoints close to the epicenter located deeper inland in “Valle de la Estrella” (see Figure 1). The motivation of this study is to provide a comprehensive compilation and evaluation of datapoints to contribute to future related modeling efforts. Also, a technique is described of how deformation values can still be computed from the Costa Rican height system.

METHODOLOGY¹

The focus of the article is to assess the quality and compile a georeferenced point collection of deformation on the vertical component in the area of interest (AOI) shown by Figure 1. The term harmonized point collection refers to the compatibility of coordinate reference systems and vertical deformation data, defined as the difference in meters between measurements of vertical component taken before and after an event.

Also, special attention is paid to knowing whether this deformation is still present today or has been elastically compensated for three decades after the co-seismic deformation. To address this first point, a compilation and evaluation of the historical sources was done searching for reports, articles and project products produced by several institutions such as the National Registry, Costa Rican Electricity Institute (ICE), The Volcanological and Seismological Observatory of Costa Rica (OVSI-CORI) and former researchers involved in the Costa Rica and Lower Saxony project (CoRBaS in Spanish abbreviation). In this latter project, researchers aimed to create a new geodetic reference system and to determine crustal deformation; campaigns were carried out in 1991 and 1993, having the 1991 campaign surveyed before the earthquake.

Furthermore, in the review of historical records, special attention was given to details of survey methods and coordinates to properly normalize and provide accuracy

¹ AI was used to just revise wording and grammar.

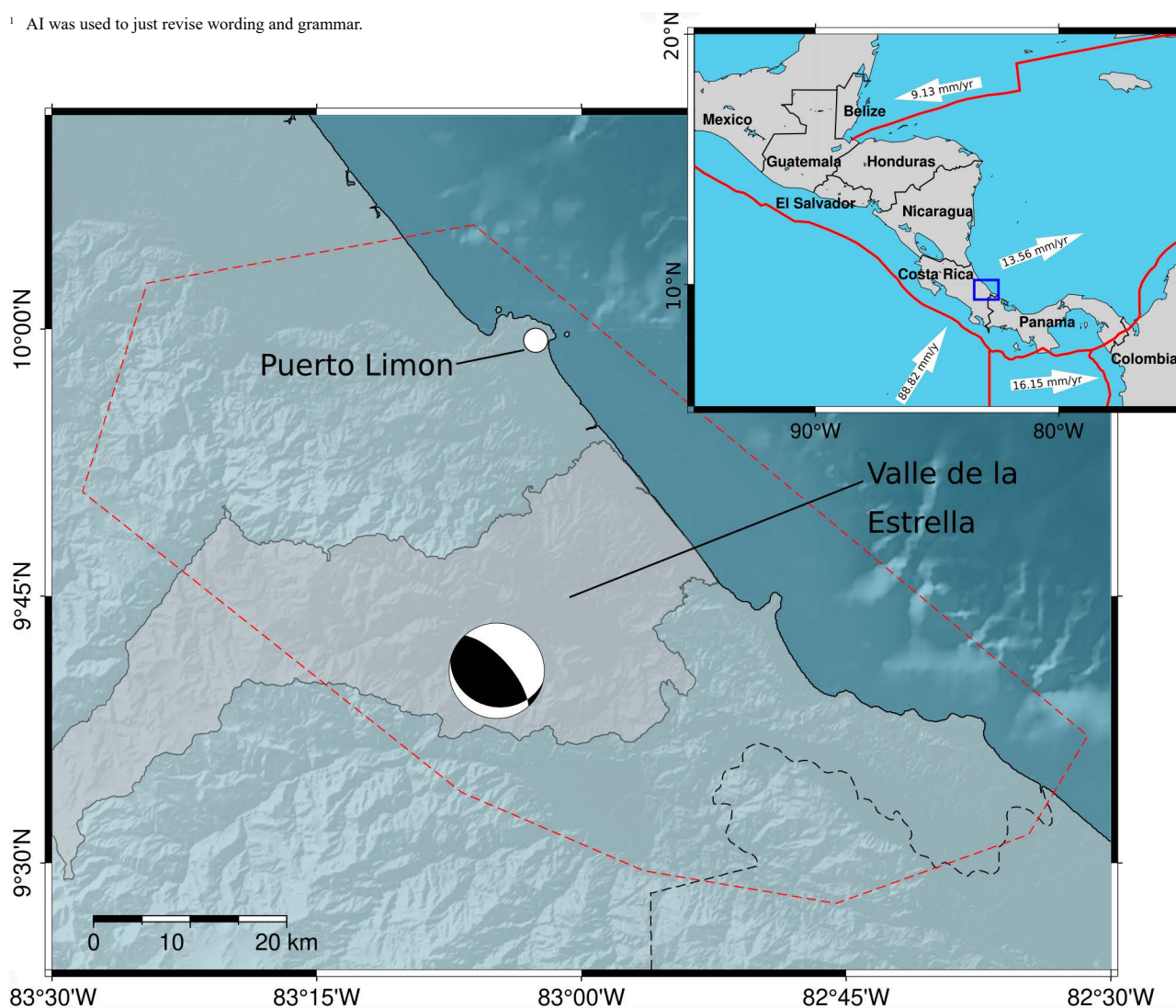


Figure 1. The white circle represents the Limon Area while the red dashed line the area of interest (AOI) for the Limon Earthquake deformation. The Location of the epicenter is represented by the focal mechanism from GCMT. The Valle de la Estrella is shaded in light grey. Plate motion rates from DeMets et al. (2010) are shown in the inset.

and reliability for each point. Moreover, coordinate system transformations from Lambert Conformal Conic Costa Rica North (EPSG: 5456) to WGS84 (EPSG: 4326) were carried out using official routines (Geotecnologías, 2016). Consequently, accuracies were estimated for each point using information provided by source articles and reports or computed standard deviations (σ).

When computing deformation from coordinates such as absolute height values, one must account for the reference of each height system, which can also be combined with inaccuracies such as the ones caused by geoid interpolations or GNSS atmospheric effects. These effects can be summarized in a bias term that makes direct comparison from absolute heights inaccurate, since this quantity cannot be separated from the deformation (See Figure 2A). This is mathematically described by Equation 1.

$$\delta + bias = Ha_{t_2} - Ha_{t_1} \quad 1$$

Where:

δ : is deformation;

Ha_{t_2} and Ha_{t_1} : are the absolute height of a benchmark (BM) at time 2 and 1 respectively, and the term bias includes aleatory and systematic errors and the difference in height reference surfaces.

However, as shown by previous research such as Obaldía et al., (1991), this seismic event affected areas along the Caribbean Coast up to Puerto Limón. A few kilometers north of this city, there were no instances of deformation reported. Moreover, when benchmarks located in the Central Costa Rica Zone and Liberia are assumed to be unaffected, the value of deformation can be computed by taking a reference benchmark (BM) and computing the double difference between an unaffected BM and one in the deformation zone (see Figure 2B). This process is shown in Equations 2 and 3.

$$\delta = [(Ha_{t_2} + bias_1) - (Hb_{t_2} + bias_1)] - [(Ha_{t_1} + bias_2) - (Hb_{t_1} + bias_2)] \quad 2$$

$$\delta = \Delta H_{t_2} - \Delta H_{t_1} \quad 3$$

Where:

δ : is deformation;

Ha_{t_2} and Ha_{t_1} : are the absolute heights of a benchmark (BM) located inside the deformation zone at times 2 and 1, respectively;

Hb_{t_2} and Hb_{t_1} : are the absolute heights of a benchmark (BM) located outside the deformation zone at times 2 and 1, respectively;

$bias_2$ and $bias_1$: are errors in absolute height measurements at times 2 and 1, respectively.

Figure 2 shows a schematic of deformation computation from the altimetric benchmarks.

In our study, the x, y, z components between reference points are the vectors of CoRBaS 9091 and CoRBAS 93 (before and after earthquake, respectively). These vectors were analyzed to find extra information from the event and replicate the results from Lundgren et al. (1993). A set of reference stations outside the affected area was chosen (Liberia, Acosta, ETCG, Uvita, Campos) (see Figure 3). These stations had two characteristics: they were present in both field surveys 90 – 91 and 93, and were connected to points in the affected zone by a vector. To decrease variability and limit uncertainty propagation, a least squares adjustment (LSA) — see Ghilani (2017) — was first performed over these reference stations, including measurements of the two campaigns. Since these points are assumed to be unaffected by the earthquake one reference station was evaluated with a fixed height value (Liberia) Secondly, another LSA was performed, having the reference station fixed and adjusting the vectors of the points on the affected areas. Then, the difference is computed to get deformation values. Figure 3 shows the distribution of stations of the Costa Rican geodetic system and the points that fall into the area of interest (AOI).

A similar process is performed to compare the altimetric height system before and after this event. 5 benchmark points were used to compute a barycenter instead of relying solely on one point. Then, we used this barycenter to estimate a deformation in each point, in order to ensure that

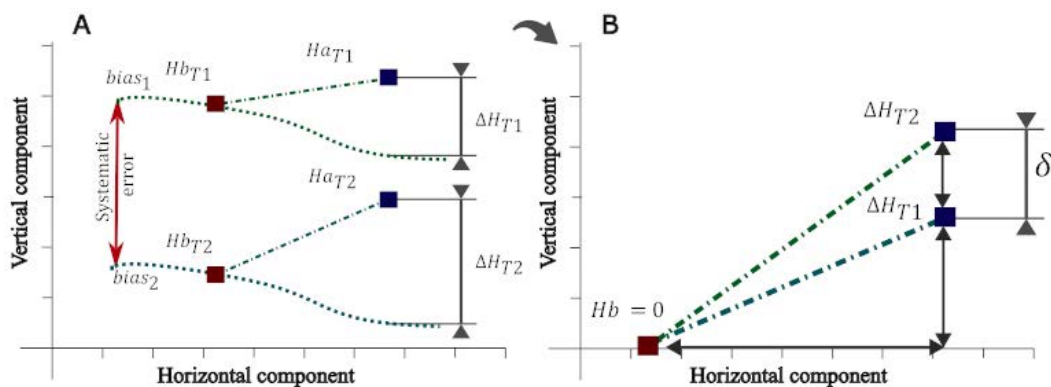


Figure 2. Graphical representation of the deformation calculation (δ). Hb_{t_1} and Hb_{t_2} correspond to a point that has not been deformed by the event. Hb represents the new reference height after transformation which is equal to 0.

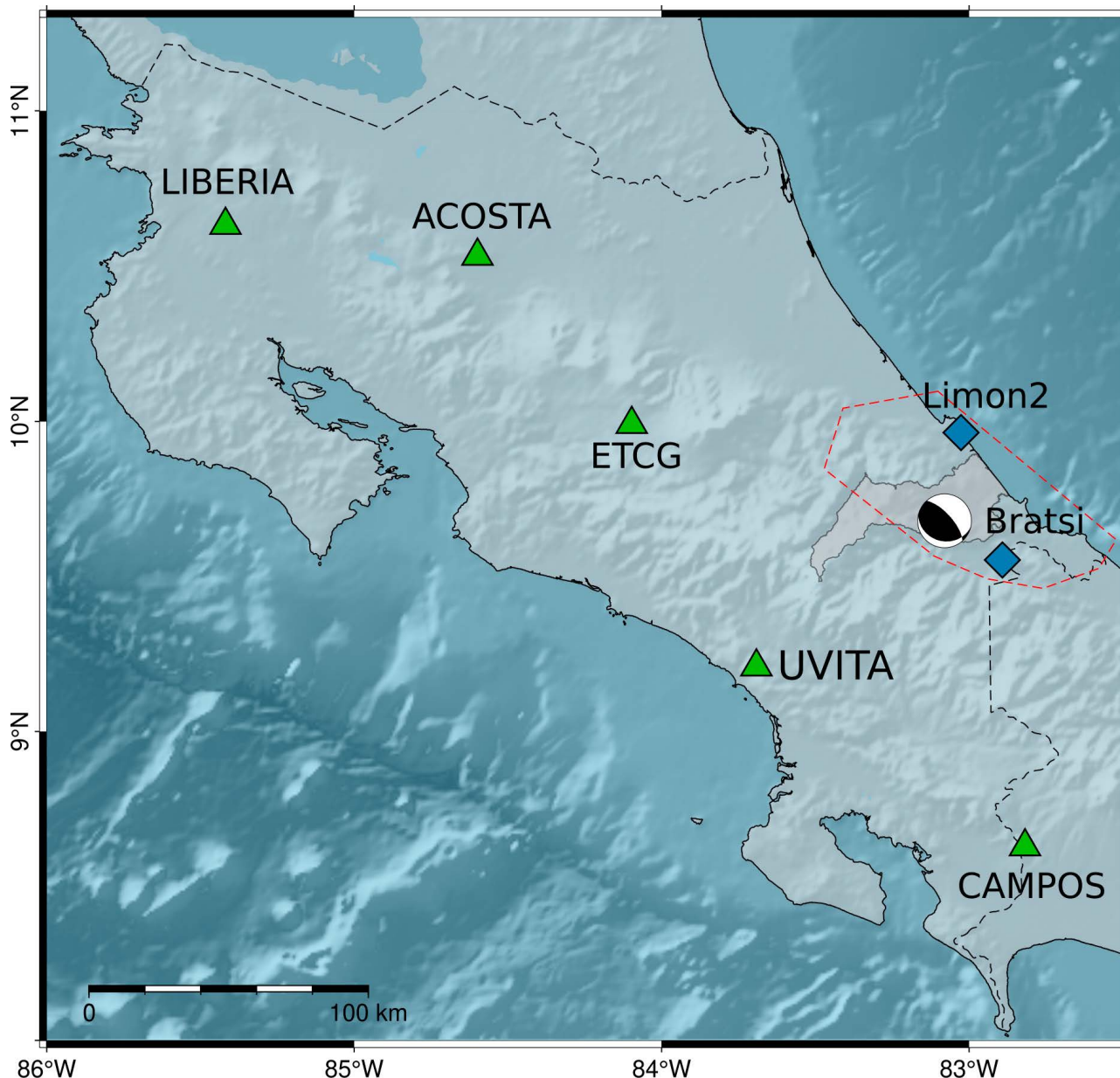


Figure 3. Distribution of the stations for the Costa Rican geodetic system, diamond markers in blue show points of interest within the deformation zone, while triangle markers in green show reference stations outside of the co-seismic deformation area. The focal mechanism represents the epicenter and the surrounding grey zone the Valle de la Estrella region.

there were no outliers, and to compute a standard deviation as a parameter of significance. For data before 1991, heights are taken from the original benchmark records. On the other hand, for 2020, the heights are measured using GNSS and converted to physical height using the GCR_RSH_2020 (Garbanzo-León et al., 2020) Then, taking this barycenter as reference, the process shown by figure 2 was performed. It is worth noting that the original height values were determined in surveys conducted in the 1960's and 1970's, prior to the main co-seismic deformation event for the area. These values represent an epoch that will be referred to as T-1991 in this study.

Finally, we compared the z deformation dataset (T-1991) compiled from historical sources. This last com-

parison is computed solely on the benchmarks (BMs) of the altimetric network, with deformation estimated from GNSS and original heights (T-2020). Because the point density and location differ between datasets, a spatial aggregation was performed on T-1991. This aggregation consisted of a mean value over grid of 5 km resolution, which was chosen because it reduces the number of points to a similar quantity for T-2020. Moreover, this grid was used to compute a raster using a triangulated irregular network tool (TIN). Then, this final product was used to estimate the values on the point location of the current T-2020. Consequently, we compared these deformation quantities.

RESULTS

In the historical research phase, we found that only 7 independent sources contained useful vertical deformation information. A total of 113 data points were retrieved, which were composed of 111 points coming from direct observations and 2 points extracted from 29 GNSS observations produced by the CoRBaS project. From these sources, 4 different survey methods were found: trigonometric leveling, hand leveling, GNSS, and an undetermined method described as “large-scale deformation observations”.

The more robust methods in terms of accuracy and confidence are GNSS and trigonometric leveling; GNSS observations tend to have higher error on measurements, but these are global, in the sense that these errors are not much affected by the distance of the baseline and are referred to a global terrestrial reference frame. In contrast, trigonometric leveling errors are relative and accumulative, which means that uncertainties will increase with the distance. Moreover, the operator must change position often

and this can lead to mistakes while setting up equipment. Hand leveling is the most imprecise method, which produces quick level differences measurements but does not allow for the calculation of uncertainties or quality control. Also, the deformations taken with this last method refer to the apparent mean sea level and the exposure to intertidal organisms such as barnacles and calcareous sea worms.

This reference level can be subjective and relative to the observer’s criteria. Researchers estimated the errors of these measurements to be between 20 to 30 cm (Plafker, 1992; Denyer et al., 1994). The fourth class was identified as undetermined method or large-scale deformation observations; these were classified as such when there was no clear description of a survey methods for the deformation observation, or these were based on estimates using large scale observations like comparisons of historical maps, field observations, historical photographs and others.

To further evaluate these methods, we estimated a range of uncertainty based on 2σ for trigonometric leveling and GNSS results, with 5 and 15 cm respectively. Also, we

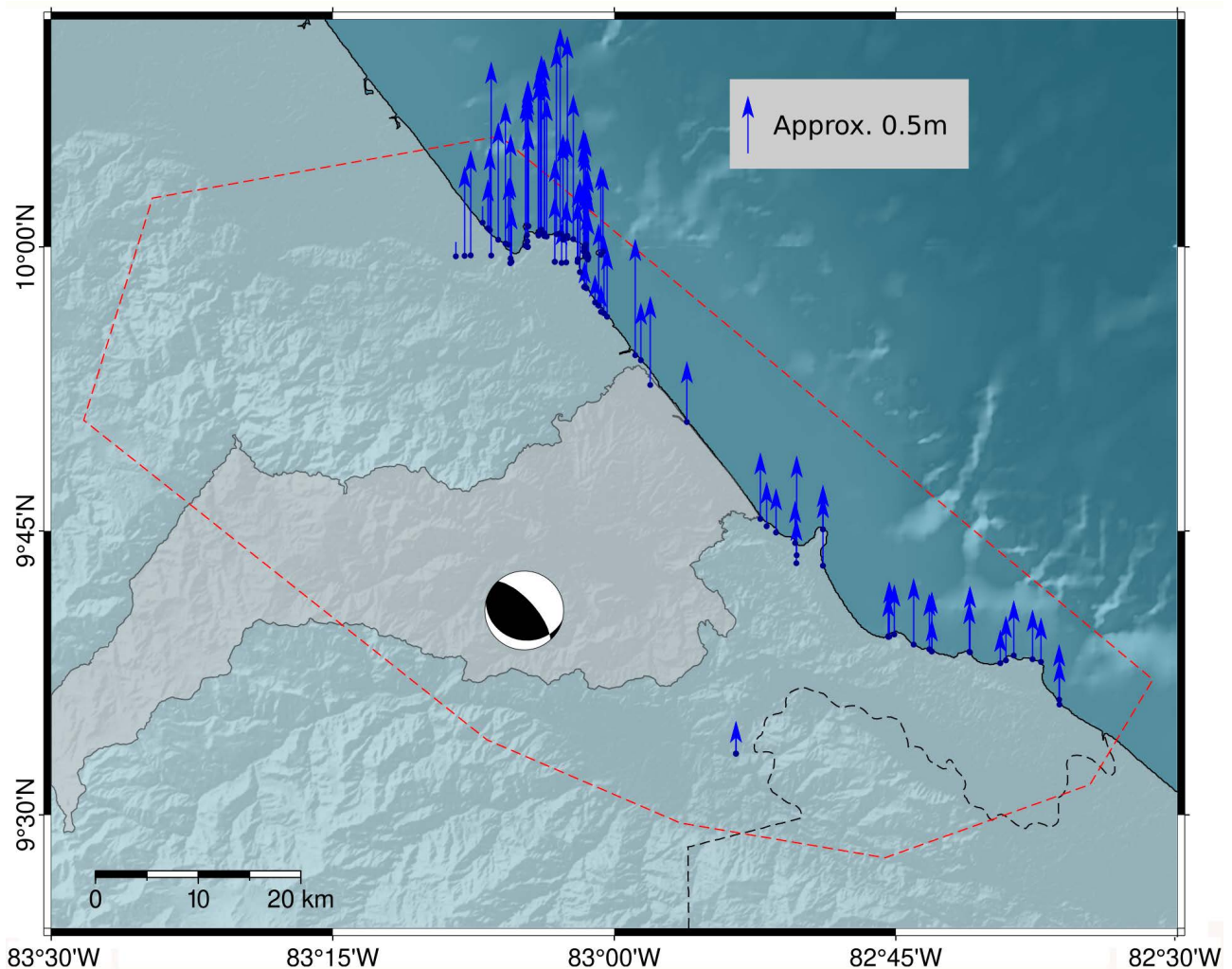


Figure 4. distribution of historical dataset of deformation from the period T-1991 and its approximate deformation magnitude. The light grey zone represents Valle de la Estrella while the focal mechanism marks the epicenter. Stippled red line marks the area of interest. Stippled black line marks the border between Costa Rica and Panama.

concluded that the errors reported by authors are an adequate estimate (approx. 20 cm) for hand leveling. Finally, we assigned an accuracy of 30 cm for the class representing undetermined method or large-scale deformation observations. One can notice that 30 cm is a very low accuracy but because of the order of deformation occurred in this event is on the metric level, this is still significant. Table 1 summarizes the reported values and Figure 4 shows the distribution and magnitude of the deformation for the historical dataset.

The CoRBaS campaigns (CoRBaS9091 and CoRBaS93) were analyzed by Dörries and Roldan (1999), who provided detailed and useful reports of observations. From these reports, only 2 points (BRATSI and LIMON2) of the geodetic network have information in the two periods T-1991 and T-1993 and therefore can provide deformation values within the zone of co-seismic deformation (See Figure 3). These deformation values have a magnitude of 0.39 and 0.31 m respectively (see Table 2). Moreover, Lundgren et al (1993) reported values of 0.15 and 0.16 m respectively. These last 2 quantities are more reliable because deformation values were obtained in surveys targeting this event. However, the values shown in Table 2 have other reference stations vectors included and show a positive deformation. Thus, these deformation values can also increase the degrees of freedom in a deformation model.

Table 1. Estimation of accuracy by method and hierarchy of confidence

Survey method	Estimated uncertainty (2 σ) (m)	Precision score
Trigonometric leveling	± 0.05	High
GNSS	± 0.15	Medium
Hand leveling	± 0.20	Low
Undetermined method or large-scale deformation observations	± 0.30	Very low

Table 2. Deformation computed from the two CoRBaS campaigns (CoRBaS9091 and CoRBaS93)

Station	Deformation (m)	σ (m)
BRATSI	0.39	± 0.05
LIMON2	0.31	± 0.04

Table 3. Benchmarks (BMs) used for the barycenter computation.

BM Code	Source	Lon (deg)	Lat (deg)	N GCR_RSH_2020 (m)	H (bf. 1991) (m)	h (2020) (m)	H (2020) (m)	Biased Diff (m)
160	G1	-83.64464	10.19546	11.84	74.46	86.14	74.30	-0.16
105B	G1	-83.68393	9.90572	15.08	645.98	660.90	645.82	-0.16
161	C&L	-83.67876	10.20846	11.83	99.31	111.00	99.17	-0.15
154	*	-83.53723	10.12300	12.14	100.42	112.30	100.16	-0.26

Current deformation on benchmark (BMs)

4 BMs (shown in Table 3) were chosen for the barycenter computation because they are outside the affected area. The bias between the reference surfaces can be seen in the column of the biased difference, which is on average -0.18 m with a standard deviation of 0.06 m. This means that the two surfaces are consistently separated and there is not a high deformation among points, which show surprising results considering that heights measurements have a time span between 60 and 40 years. Figure 5 presents the distribution of BMs within both the AOI and the reference area used for barycenter calculation.

Table 4 shows the computed barycenter with the 2 values for both epochs, 1991 and 2020. Also, it shows the differences once the barycenter is used to transform the values to unbiased level differences from the datasets, T-1990 and T-2020. As these differences are at the centimeter level, it can be concluded that these points did not have significant deformation in the last three decades, and that the Limon earthquake did not deform the height difference among these 5 benchmarks.

Over the last 3 decades, many of the altimetric network of Costa Rica BMs have been lost consistently because vandalism, new infrastructure building, and weather conditions. Thus, these BMs have become a scarce resource, and many of the ones used in past deformation studies are lost. However, from Obaldía et al. (1991), 3 deformations points could be extracted and compared to new deformation computations, the results are presented in Table 5. This table shows that the deformation signal is still present in the altimetric system. Although these differences are positive, the quantities are within the 2-sigma range of the barycenter and GNSS measurement uncertainty combination, therefore, they should not be considered significant.

Finally, a table with the current deformation on the BMs (T-2020) was compiled with 16 datapoints. From these deformation values, 13 of them are positive and 3 negative. These negative values are located near bridges and rivers and, therefore, are more likely a consequence of liquefaction [see Camacho and Viquez (1994) and Denyer (1994)]. Moreover, these results show that points on bridge abutment are not fit for placing BMs.

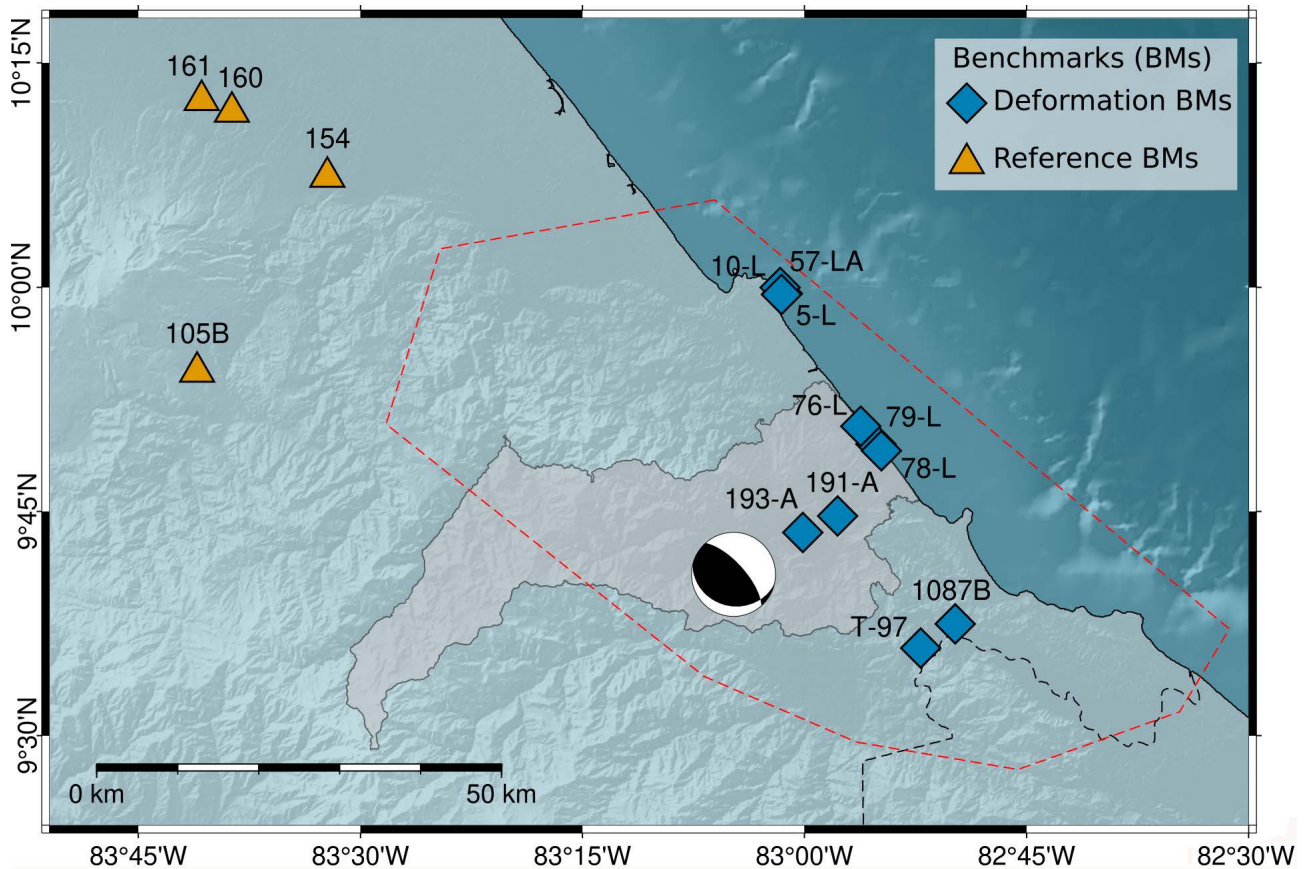


Figure 5. Distribution of the Benchmarks (BMs) within the deformation zone (blue diamonds) and the reference stations BMs (orange triangles), which were used to compute the barycenter. Focal mechanism marks the epicenter. Stippled red line marks the area of interest. Stippled black line marks the border between Costa Rica and Panama.

Table 4. Barycenter computation and unbiased differences of the reference benchmarks.

	Lat (deg)	Lon (deg)	H (T-1991) (m)	H (T-2020) (m)	Biased Diff (m)	Sigma (m)
Barycenter	10.10816	-83.63614	230.04	229.86	-0.18	0.06
BN	Unbiased (diff) (m)					
160	0.03	-	-	-	-	-
105B	0.02	-	-	-	-	-
161	0.04	-	-	-	-	-
154	-0.08	-	-	-	-	-

Table 5. Deformation differences between deformation values from Obaldía et al. (1991) and the current deformation on 3 BMs of the altimetric network.

BM	Deformation Obaldía et al. (1991) (m)	Deformation 2020 – GNSS-geoid (m)	Differences
5L	0.64	0.78	+ 12 cm
10L	0.92	1.05	+ 13 cm
57 LA	0.69	0.86	+ 17 cm

Comparison between deformation from the year T-2020 To T-1991

Using the harmonized triangulated information from T-1991, the 12 points with positive deformation values were interpolated. Consequently, the result of this computation had two deformation values for T-1991 and T-2020. A total of 10 points were used for this comparison after outlier removal. Both deformation values, T-1991 and T-2020 showed a significant uplift of 57 and 48 cm, with standard deviation of 7 and 9 cm respectively. These numbers show that a significant subsidence of 10 cm on average (P-value of 0.03) occurred since the event in 1991. Table 6 below shows a comparison of the main statistics for both times.

Figure 6 shows the different BMs and a clear correlation of the deformation values. Also, BMs in the Puerto Limon Area (10 L, 5 L, 57-LA) appear to be more stable. However, the remaining BMS contain most of the magnitude of relaxation. Although long term viscoelastic relaxation is still possible (Wang et al., 2012), the decay of after slip and viscoelastic deformations has been measured in a range between 2 to 2.5 years after the event (Ozawa et al., 2012;

Table 6. Summary of the main statistics from the comparison between periods T-1991 and T-2020.

	T-1991	T-2020
N	10	
Mean (m)	0.57	0.48
STD (m)	0.07	0.10
Max (m)	0.87	1.05
Min (m)	0.26	0.04

Yamagiwa et al., 2015). Thus, there is a high probability that the deformation shown for T-2020 is permanent.

The result of this paper proves that the Costa Rica height network still contains part of the deformation signal from the 1991 Limon earthquake. Thus, a deeper BMs search inland, towards the west, could help to characterize the regional deformation and its extent more precisely. Furthermore, we provide the full extent of the information found for both T-1991 and T-2020 (See Annex 1 and 2), including the negative values to let the future researcher decide whether they should be considered in their research. We believe this is a valuable contribution to future research on the dynamics of this area.

CONCLUSION

We performed a thorough historical search to find z deformation values with the objective of compiling a unified dataset. A total of 113 datapoints were compiled from 7 different sources. Also, we reprocessed the network coordinate system data from the GNSS based survey campaigns of CoRBaS9091 and CoRBaS93, which also show an uplift as in Lungren et al. (1993). These latter measurements added some degrees of freedom to the current deformation information in the z coordinate. Although some historical information in government institutions might still exist, it is more likely to be archived with other unrelated information and thus may not be accessible.

Moreover, a technique was tested to extract deformation information for this event from the altimetric system during this project; the results showed a general positive uplift. However, only long-lasting deformation can be

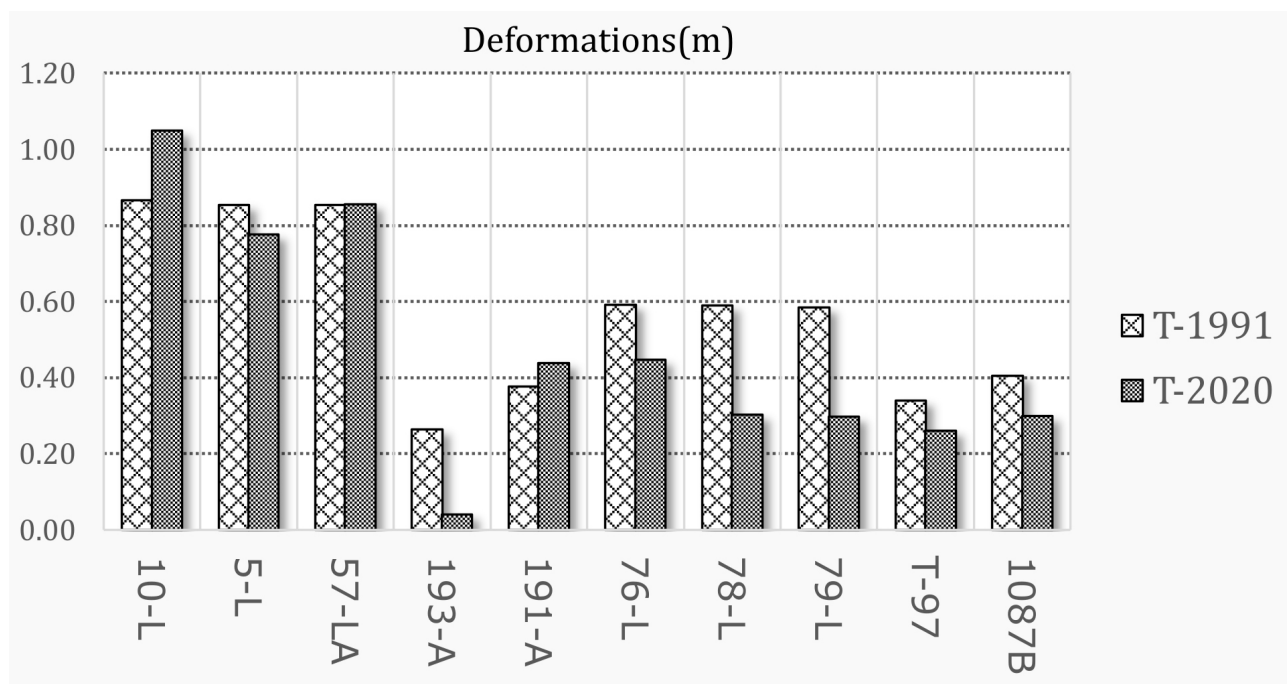


Figure 6. Comparison of positive vertical deformation magnitudes for the periods T-1991 and T-2020. Deformation values are shown in meters.

retrieved with this technique because it needs GNSS measurement over benchmarks which are not available and must be surveyed. However, when comparing T-1991 and T-2020, we found that most of the deformation signal is still present on the Costa Rican height system in spite of the presence of post-seismic subsidence related to elastic deformation during the three decades after the main co-seismic slip. This result is important because it could contribute to the understanding of what the long-term effects of this event are deeper inland towards the west, in the case that additional BMs can be found. Also, these datasets should be analyzed and modeled to understand how they improve the current solutions and to find a deformation and fault slip model over the region.

REFERENCES

- Adamek, S., Frohlich, C., Pennington, W. (1988). Seismicity of the Caribbean-Nazca Boundary Constraints on Microplate Tectonics of the Panama Region. *Journal of Geophysical Research*, 93(B3), 2053-2075.
- Amador, J. A., Chacón, R. E., Lizano, O. G. (1994). Estudio de efectos geofísicos del Terremoto de Limón mediante percepción remota y análisis hidrometeorológico. *Revista Geológica de América Central*. Available at: <https://archivo.revistas.ucr.ac.cr//index.php/geologica/articulo/view/13448/12703>. Accessed on: Aug 28, 2025.
- Barrantes, G., Vahrson, W. G., Mora, S. (2021). Cambios geomorfológicos e hidrológicos inducidos por el terremoto (Mw 7, 7) del 22 de abril de 1991 en la provincia de Limón, Costa Rica. *Revista Geológica de América Central*, 65, 1–19. <https://doi.org/10.15517/rgac.v0i65.46881>
- Camacho, E., Viquez, V. (1994). Licuefacción y hundimientos costeros en el noroeste de Panamá durante el Terremoto de Limón. *Revista geológica de América central*. Available at: <https://dialnet.unirioja.es/servlet/articulo?codigo=6319126>. Accessed on: Sep 06, 2025.
- Chacón-Barrantes, S., Zamora, N. (2017). Numerical Simulations of the 1991 Limón Tsunami, Costa Rica Caribbean Coast. *Pure and Applied Geophysics*, 174(8), 2945–2959. <https://doi.org/10.1007/s00024-017-1631-x>
- Cordero, G., Lara, G. (2023). Determinación de coordenada elipsoidal y Gravedad relativa a los bancos de nivel identificados de costa Rica.
- DeMets, C., Gordon, R. G., Argus, D. F. (2010). Geologically current plate motions. *Geophysical Journal International*, 181, 1-80. <https://doi.org/10.1111/j.1365-246X.2009.04491.x>
- Denyer, P., Arias, O., Personius, S. (1994). Efecto tectónico del terremoto de Limón. *Revista Geológica de América Central*. Available at: <https://scispace.com/pdf/efecto-tectonico-del-terremoto-de-limon-58b8nflia2.pdf>. Accessed on: Aug 28, 2025.
- Dörries, E., Roldán, J. (1999). *Estudio comparativo del datum geodésico de Ocotepaque y el datum satelitario del sistema WGS84*. Informe Final Del Proyecto de Investigación, Escuela de Topografía, Catastro y Geodesia. Heredia, Costa Rica: Facultad de Ciencias Exactas y Naturales, Universidad Nacional.
- Dörries, E., Roldán, J. (2004). El datum geodesic de Ocotepaque y el datum satelitario del sistema WGS84. *Uniciencia*. Available at: <https://repositorio.una.ac.cr/items/b4a462b7-110e-4244-af05-7bbe6112ec45/full>. Accessed on: Sep 01, 2025.
- Dziewonski, A. M., Chou, T. A., Woodhouse, J. H. (1981). Determination of earthquake source parameters from waveform data for studies of global and regional seismicity. *Journal of Geophysical Research: Solid Earth*, 86, 2825-2852. <https://doi.org/10.1029/JB086iB04p02825>
- Ekström, G., Nettles, M., Dziewoński, A. M. (2012). The global CMT project 2004–2010: Centroid-moment tensors for 13,017 earthquakes. *Physics of the Earth and Planetary Interiors*, 200-201, 1-9. <https://doi.org/https://doi.org/10.1016/j.pepi.2012.04.002>.
- Fu, G., Zhao, J., Liu, T., Gao, S., Wang, Z. (2025). Spatio-temporal evolution of post-seismic deformation caused by large earthquakes around the Pacific and its impact on plate movement. *Geophysical Journal International*, 240(1), 201-211. <https://doi.org/10.1093/gji/ggae383>
- Garbanzo-León, J., Fernández, A. V., Sánchez, M. V., Salvatierra, J. P., Kingdon, R. W., Lücke, O. H. (2020). A regional Stokes-Helmert geoid determination for Costa Rica (GCR-RSH-2020): computation and evaluation. *Contributions to Geophysics and Geodesy*, 50(2), 223-247. <https://doi.org/10.31577/congeo.2020.50.2.3>
- Geotecnologías (2006). *Transformación de Coordenadas Entre Sistemas de Referencia*. Informe Técnico N° 14 para la definición y oficialización del sistema de coordenadas. San José, Costa Rica: Registro Nacional de la República de Costa Rica.
- Ghilani, C. D. (2017) *Adjustment computations: spatial data analysis*. Hoboken, New Jersey: John Wiley & Sons. <https://doi.org/10.1002/9781119390664>
- Lundgren, P. R., Kornreich Wolf, S., Protti, M., Hurst, K. J. (1993). GPS measurements of crustal deformation associated with the 22 April 1991, Valle de la Estrella, Costa Rica earthquake. *Geophysical Research Letters*, 20(5), 407-410. <https://doi.org/10.1029/93GL00294>
- Monge, R. (1991). Medición de la red nacional de coordenadas con equipo de georecepción de satélites. *Revista Del Colegio Federado de Ingenieros y Arquitectos*, 34, 26-30. Available at: <https://revista.cfia.or.cr/wp-content/uploads/2018/03/revista34-5.pdf>. Accessed on: Aug 28, 2025.

- Niemeier, W. W., Roldan, J., Aguilar, L., Pelzer, H., Bagge, A., Augath, W., Seifert, W. (1993). The project CORBAS—Determination of recent crustal movements in Costa Rica. In: W. Torge et al. (eds.) *Recent Geodetic and Gravimetric Research in Latin America*. 146-156. Berlin: Springer. Available at: https://link.springer.com/content/pdf/10.1007/978-3-642-88055-1_12.pdf. Accessed on: Aug 28, 2025.
- Obaldía, F., Marino, T., Van Der Laat, R., Malavassi, E., Hernandez, F., Morera, R., Trejos, F., Slattery, K., Mc Nally, K. C. (1991). *Levantamiento cosísmico asociado al terremoto del 22 de abril de 1991, Ms=7.5 Valle de la Estrella, Limón, Costa Rica Parte I*. Heredia, Costa Rica: Universidad Nacional. Observatorio Vulcanológico y Sismológico de Costa Rica. Available at: <https://pesquisa.bvsalud.org/portal/resource/pt/des-2808>. Accessed on: Aug 28, 2025.
- Ozawa, S., Nishimura, T., Munekane, H., Suito, H., Kobayashi, T., Tobita, M., Imakiire, T. (2012). Preceding, coseismic, and postseismic slips of the 2011 Tohoku earthquake, Japan. *Journal of Geophysical Research: Solid Earth*. <https://doi.org/https://doi.org/10.1029/2011JB009120>
- Plafker, G., Ward, S. N. (1992). Backarc thrust faulting and tectonic uplift along the Caribbean Sea coast during the April 22, 1991 Costa Rica earthquake. *Tectonics*, 11(4), 709-718. <https://doi.org/10.1029/92TC00609>
- Quesada-Román, A. (2016). Impactos geomorfológicos del Terremoto de Limón (1991; ms= 7.5) y consideraciones para la prevención de riesgos asociados en Costa Rica. *Revista Geográfica de América Central*, 1(56), 93-111. <https://doi.org/10.15359/rgac.1-56.4>
- Rodríguez-Roblero, M. J., Lobo-Aguilar, S., Vargas-Alas, L. G., Castillo-Barahona, R. (2021). Impacto del terremoto de Limón de 1991 en el diseño estructural de puentes. *Revista Geológica de América Central*, 65, 430-446. <https://doi.org/10.15517/rgac.v0i65.46880>
- Sauter, F. (1994). Evaluación de daños en puentes y otras estructuras civiles causados por el terremoto de Limón. *Revista Geológica de América Central*. Available at: <https://hdl.handle.net/10669/22548>. Accessed on: Aug 28, 2025.
- Soulas, J. P. (1991). El sismo de Limón-Changuinola (Costa Rica y Panamá) del 22 de abril de 1991. *Communities & Collections*, 1-13. Available at: <https://www.cne.go.cr/cedo-crid/pdf/spa/doc656/doc656-contenido.pdf>. Accessed on: Jan 14, 2026.
- U.S. Geological Survey. (n.d.). *Significant Earthquakes - 1991*. Available at: <https://earthquake.usgs.gov/earthquakes/browse/significant.php?year=1991>. Accessed on: 19 Feb. 2025.
- U.S. Geological Survey. (2014). *M 7.6 - 34 km S of Limón*, Costa Rica. Available at: <https://earthquake.usgs.gov/earthquakes/eventpage/usp0004qpg/origin/detail?source=us&code=usp0004qpg>. Accessed on: 19 Feb. 2025.
- Wang, K., Hu, Y., He, J. (2012). Deformation cycles of subduction earthquakes in a viscoelastic Earth. *Nature*, 484(7394), 327–332. <https://doi.org/10.1038/nature11032>
- Yamagiwa, S., Miyazaki, S., Hirahara, K., Fukahata, Y. (2015). Afterslip and viscoelastic relaxation following the 2011 Tohoku-oki earthquake (Mw9.0) inferred from inland GPS and seafloor GPS/Acoustic data. *Geophysical Research Letters*, 42(1), 66-73. <https://doi.org/https://doi.org/10.1002/2014GL061735>

ATTACHMENTS

Annex 1. Deformation table at T-1991 by method and source.

INDEX	NAME	LAT	LON	DEF. (m)	σ (m)	Method	Source
1	NA	10.03691	-83.12973	0	0.2	HL/DL	1
2	NA	10.02136	-83.11695	0.15	0.2	HL/DL	1
3	NA	10.01636	-83.11223	0.44	0.2	HL/DL	1
4	NA	10.01469	-83.11057	0.74	0.2	HL/DL	1
5	NA	10.00636	-83.10307	1.06	0.2	HL/DL	1
6	NA	10.00303	-83.09668	1.27	0.2	HL/DL	1
7	NA	10.00108	-83.0789	1.34	0.2	HL/DL	1
8	NA	10.00497	-83.07723	1.4	0.2	HL/DL	1
9	NA	10.01025	-83.07751	1.25	0.2	HL/DL	1
10	NA	10.0183	-83.0764	0.88	0.2	HL/DL	1
11	NA	10.0183	-83.0764	1.2	0.2	HL/DL	1
12	NA	10.0183	-83.0764	0.9	0.2	HL/DL	1
13	NA	10.01414	-83.06584	1.43	0.2	HL/DL	1
14	NA	10.01191	-83.06223	1.57	0.2	HL/DL	1
15	NA	10.00941	-83.06196	1.42	0.2	HL/DL	1
16	NA	10.00914	-83.06001	1.24	0.2	HL/DL	1
17	NA	10.00942	-83.04557	0.92	0.2	HL/DL	1
18	NA	10.00636	-83.04557	0.9	0.2	HL/DL	1
19	NA	10.00192	-83.02557	0.99	0.2	HL/DL	1
20	NA	10.00192	-83.02557	1.01	0.2	HL/DL	1
21	NA	9.99608	-83.02723	1	0.2	HL/DL	1
22	NA	9.99608	-83.02723	1.1	0.2	HL/DL	1
23	NA	9.99358	-83.0239	0.78	0.2	HL/DL	1
24	NA	9.99108	-83.02307	0.4	0.2	HL/DL	1
25	NA	9.99108	-83.02307	0.6	0.2	HL/DL	1
26	NA	9.97775	-83.03057	0.84	0.2	HL/DL	1
27	NA	9.96359	-83.02473	0.72	0.2	HL/DL	1
28	NA	9.94831	-83.0139	0.74	0.2	HL/DL	1
29	NA	9.93859	-83.0064	0.62	0.2	HL/DL	1
30	NA	9.90026	-82.9764	0.52	0.2	HL/DL	1
31	NA	9.73944	-82.83946	0.38	0.2	HL/DL	1
32	NA	9.71944	-82.81473	0.73	0.2	HL/DL	1
33	NA	9.65666	-82.75668	0.38	0.2	HL/DL	1
34	NA	9.65889	-82.7514	0.45	0.2	HL/DL	1
35	NA	9.64389	-82.71807	0.54	0.2	HL/DL	1
36	NA	9.64389	-82.71807	0.29	0.2	HL/DL	1
37	NA	9.64361	-82.68474	0.45	0.2	HL/DL	1
38	NA	9.63361	-82.65724	0.3	0.2	HL/DL	1
39	NA	9.63611	-82.65224	0.4	0.2	HL/DL	1
40	NA	9.59722	-82.60474	0.4	0.2	HL/DL	1
41	NA	10.07635	-83.16057	0	0.2	HL/DL	2
42	NA	10.02497	-83.1189	0	0.2	HL/DL	2
43	NA	10.00192	-83.0939	0.6	0.2	HL/DL	2

44	NA	9.99997	-83.07668	1.5	0.2	HL/DL	2
45	NA	10.01108	-83.06751	1.4	0.2	HL/DL	2
46	NA	10.01247	-83.06473	1.6	0.2	HL/DL	2
47	NA	10.01525	-83.06473	1.5	0.2	HL/DL	2
48	NA	10.01108	-83.0514	1.7	0.2	HL/DL	2
49	NA	10.01191	-83.04807	1.85	0.2	HL/DL	2
50	NA	10.00969	-83.04168	1.8	0.2	HL/DL	2
51	NA	10.00692	-83.0364	1.3	0.2	HL/DL	2
52	NA	9.99775	-83.02584	0.9	0.2	HL/DL	2
53	NA	9.99303	-83.01196	0.8	0.2	HL/DL	2
54	NA	9.9958	-83.01001	0.75	0.2	HL/DL	2
55	NA	9.98886	-83.02362	0.8	0.2	HL/DL	2
56	NA	9.94164	-83.00918	0.7	0.2	HL/DL	2
57	NA	9.9047	-82.9814	1.05	0.2	HL/DL	2
58	NA	9.84582	-82.93557	0.55	0.2	HL/DL	2
59	NA	9.76055	-82.87029	0.6	0.2	HL/DL	2
60	NA	9.75416	-82.86473	0.4	0.2	HL/DL	2
61	NA	9.7486	-82.8564	0.4	0.2	HL/DL	2
62	NA	9.72166	-82.83835	0.4	0.2	HL/DL	2
63	NA	9.75138	-82.81473	0.3	0.2	HL/DL	2
64	NA	9.65694	-82.75585	0.5	0.2	HL/DL	2
65	NA	9.65	-82.73418	0.6	0.2	HL/DL	2
66	NA	9.64583	-82.72029	0.5	0.2	HL/DL	2
67	NA	9.64305	-82.68418	0.6	0.2	HL/DL	2
68	NA	9.64028	-82.64529	0.5	0.2	HL/DL	2
69	NA	9.63694	-82.62862	0.45	0.2	HL/DL	2
70	NA	9.63472	-82.62112	0.4	0.2	HL/DL	2
71	NA	9.60139	-82.60501	0.5	0.2	HL/DL	2
72	NA	9.87859	-82.96807	0.8	0.3	OTHERS	3
73	NA	9.7286	-82.83807	0.9	0.3	OTHERS	3
74	NA	9.53459	-82.58408	-1	0.3	OTHERS	4
75	NA	9.45903	-82.43602	-0.3	0.3	OTHERS	4
76	NA	9.40431	-82.32602	-0.9	0.3	OTHERS	4
77	NA	9.33987	-82.23602	-0.5	0.3	OTHERS	4
78	LIMO	9.96467	-83.02667	0.16	0.0209	GNSS	5
79	BRATSI	9.5539	-82.89197	0.15	0.03	GNSS	5
80	12-L	10.00779	-83.04168	0.92	0.005	TL/WILD-T2000	6
81	10-L	9.99946	-83.02712	0.92	0.008	TL/WILD-T2000	6
82	57-LA	9.99312	-83.02487	0.69	0.01	TL/WILD-T2000	6
83	144-LA	9.99176	-83.02441	0.66	0.01	TL/WILD-T2000	6
84	5L	9.99204	-83.02596	0.64	0.011	TL/WILD-T2000	6
85	11-A	9.99131	-83.02547	0.61	0.011	TL/WILD-T2000	6
86	AYA BN-1	9.98908	-83.03236	0.67	0.012	TL/WILD-T2000	6
87	143-AC	9.98641	-83.04268	0.55	0.013	TL/WILD-T2000	6
88	143-AB	9.98598	-83.04678	0.36	0.014	TL/WILD-T2000	6
89	142-A	9.9869	-83.05271	0.92	0.015	TL/WILD-T2000	6

90	142-AB	9.9869	-83.05289	0.59	0.015	TL/WILD-T2000	6
91	S-39	10.00011	-83.07728	1.32	0.013	TL/WILD-T2000	6
92	14-L	10.01002	-83.06721	1.51	0.01	TL/WILD-T2000	6
93	S-39	10.00011	-83.07728	1.32	0.013	TL/WILD-T2000	6
94	S-34	10.03603	-83.13105	-0.01	0.02	TL/WILD-T2000	6
95	S-33A	10.0528	-83.14312	-0.55	0.022	TL/WILD-T2000	6
96	AYA BN-1	9.98908	-83.03236	0.67	0.012	TL/WILD-T2000	6
97	57-L	9.98682	-83.03264	0.55	0.012	TL/WILD-T2000	6
98	58-L	9.96501	-83.02635	0.23	0.015	TL/WILD-T2000	6
99	60-L	9.95105	-83.01711	0.25	0.015	TL/WILD-T2000	6
100	61-L	9.94289	-83.01185	0.24	0.018	TL/WILD-T2000	6
101	S-39	10.00011	-83.07728	1.32	0.013	TL/WILD-T2000	6
102	141	9.98697	-83.09124	0.49	0.016	TL/WILD-T2000	6
103	BEL-09	9.9857	-83.09239	0.79	0.016	TL/WILD-T2000	6
104	RECOPE-2	9.98993	-83.0921	1.12	0.016	TL/WILD-T2000	6
105	140-B	9.99237	-83.10933	1.75	0.017	TL/WILD-T2000	6
106	140-A	9.99242	-83.1231	-0.67	0.019	TL/WILD-T2000	6
107	139-D	9.99253	-83.12757	0.95	0.019	TL/WILD-T2000	6
108	139-C	9.99219	-83.13295	0.81	0.019	TL/WILD-T2000	6
109	139-B	9.99177	-83.1407	0.13	0.02	TL/WILD-T2000	6
110	54-L	10.01643	-83.20957	-0.79	0.024	TL/WILD-T2000	6
111	53-L	10.01797	-83.21129	-0.85	0.025	TL/WILD-T2000	6
112	LIMON 2	9.96467	-83.02667	0.31	0.04	GNSS	7
113	BRATSI	9.5539	-82.89197	0.39	0.05	GNSS	7

TL/WILD-T2000: TRIGONOMETRIC LEVELING WITH WILD T2000 + DISTOMAT D13000;

GNSS: GNSS LEVELING;

DL/HL: DIFERENCIAL LEVELING WITH HAND LEVEL.

Source:

- 1) Plafker and Ward, 1992;
- 2) Denyer et al., 1994;
- 3) Soulas, 1991;
- 4) Camacho and Viquez, 1994;
- 5) Lundgren et al., 1993;
- 6) Obaldia et al., 1991;
- 7) Dórries and Roldán, 1999.

Annex 2. Deformation T-2020 computed using height network system and GNSS/geoid measurements.

INDEX	BN	LAT	LON	DEF.(m)	σ (m)	on bridge abutment
1	69-L	9.90860	-82.98599	-0.76	0.07	1
2	57-LA	9.99311	-83.02502	0.86	0.10	0
3	53-L	10.01779	-83.21154	0.84	0.09	1
4	30-L	10.07707	-83.41156	-0.21	0.11	1
5	1087B	9.62459	-82.83042	0.30	0.10	0
6	190	9.77239	-82.93536	1.44	0.06	0
7	191-A	9.74497	-82.96279	0.44	0.06	0
8	192-A	9.73293	-82.97849	-0.62	0.06	1
9	193-A	9.72665	-83.00186	0.04	0.07	0
10	T-97	9.59762	-82.86914	0.26	0.07	0
11	10-L	9.99969	-83.02749	1.05	0.07	0
12	78-L	9.82521	-82.91969	0.30	0.12	1
13	76-L	9.84509	-82.93662	0.45	0.14	1
14	72-L	9.88498	-82.96688	0.13	0.07	1
15	5-L	9.99199	-83.02591	0.78	0.07	1
16	79-L	9.81775	-82.91337	0.30	0.06	0